THE JOURNAL OF PHYSICAL CHEMISTRY Letters

Letter

pubs.acs.org/JPCL

Ultrafast Relaxation Dynamics of the Ethylene Cation $C_2H_4^+$

André Ludwig,[†] Elisa Liberatore,[‡] Jens Herrmann,[†] Lamia Kasmi,[†] Pablo López-Tarifa,[‡] Lukas Gallmann,[†,¶] Ursula Rothlisberger,[‡] Ursula Keller,[†] and Matteo Lucchini*[,†]

[†]Department of Physics, ETH Zurich, 8093 Zurich, Switzerland

[‡]Laboratory of Computational Chemistry and Biochemistry, EPFL, 1015 Lausanne, Switzerland

[¶]Institute of Applied Physics, University of Bern, 3012 Bern, Switzerland

Supporting Information

ABSTRACT: We present a combined experimental and computational study of the relaxation dynamics of the ethylene cation. In the experiment, we apply an extreme-ultraviolet-pump/infrared-probe scheme that permits us to resolve time scales on the order of 10 fs. The photoionization of ethylene followed by an infrared (IR) probe pulse leads to a rich structure in the fragment ion yields reflecting the fast response of the molecule and its nuclei. The temporal resolution of our setup enables us to pinpoint an upper bound of the previously defined ethylene−ethylidene isomerization time to 30 ± 3 fs. Time-dependent density functional based trajectory surface hopping simulations show that internal relaxation between the first excited states and the ground state occurs via three different conical intersections. This relaxation unfolds on femtosecond time scales and can be probed by ultrashort IR pulses. Through this probe mechanism, we demonstrate a route to optical control of the important dissociation pathways leading to separation of H or H_2.

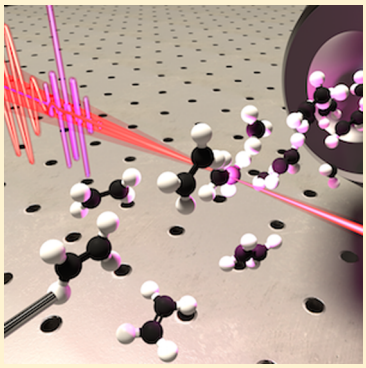

For the past several decades, photochemical reactions of the ethylene molecule (C_2H_4) and its cation have been subject to intense research because the neutral molecule serves as the simplest reference system based on a carbon double bond and the cation represents the simplest π radical system. It is known that photoexcitation of ethylene and its cation leads to ultrafast internal conversion processes and rearrangements like twisting, pyramidalization, and isomerization on the femtosecond time scale.[1−4] In particular, it has been shown that nonadiabatic coupling of the potential energy surfaces (PESs) through conical intersections (CIs) plays an important role during the evolution of the excited wave packet.[5−8] Transitions through these CIs are known to be responsible for the photochemistry of biomolecules[9−11] and for the photostability and ultraviolet (UV) resistance of DNA.[12,13]

Recently, Joalland et al.[8] conducted a theoretical study of nonadiabatic effects in the ethylene cation excited-states dynamics based on ab initio multiple spawning calculations simulations (AIMS).[5,14] They identified two distinct classes of CIs responsible for the ultrafast internal conversion and relaxation, associated with planar and twisted geometries, respectively. The role of the dissociation channels $C_2H_4^+ \rightarrow C_2H_3^+ + H$ and $C_2H_4^+ \rightarrow C_2H_2^+ + H_2$ and the underlying mechanism that influences their branching ratio has been inferred.[15,16] Specifically, the CI at the planar geometry that enables evolution to the cation ground state was associated with a bridged structure that is supposed to facilitate H migration preceding the loss of H_2. On the other hand, transitions through the twisted CI are supposed to lead to the excitation of torsional vibrations that hinder this process. According to experimental results based on a vibrationally mediated photodissociation study, it was proposed that the excitation of the vibrational mode responsible for the torsion prior to the photoexcitation can affect the branching ratio and thus the outcome of the dynamics by promoting the twisted CI. This consideration of dynamical effects extends the earlier work by Lorquet and co-workers[1,2] but challenges the role of the minimal energy configuration of the bridged and ethylidene ($HCCH_3$) structure predicted to precede the dissociation to $C_2H_2^+ + H_2$. Measurements of the dissociation dynamics on the femtosecond time scale exhibit the potential to unravel the role of the different configurations, CIs, and the excitation of vibrational modes in this process.

In contrast to theoretical studies, time-dependent experimental investigations have mostly concentrated on the V state dynamics of ethylene.[4,17−19] Recently, Tilborg et al.[20] presented results on the ethylene cation $C_2H_4^+$ dynamics obtained in an extreme ultraviolet (XUV)-pump/infrared (IR)-probe scheme similar to the one presented in this Letter. They focused on the delay of the CH_3^+ fragment yield stemming from IR-induced breakup of the C−C bond after isomerization from the ethylene to the ethylidene cation ($H_2CCH_2^+ \rightarrow HCCH_3^+$). Here, we present a combined experimental and theoretical study of the ultrafast ethylene cation excited-state dynamics with improved temporal resolution on the order of 10 fs. This temporal resolution allows us to refine an upper limit to the isomerization time, to pinpoint dynamics in a broader set of fragments, and to shed light on the branching ratio of the

Received: March 22, 2016
Accepted: May 3, 2016

DOI: 10.1021/acs.jpclett.6b00646
J. Phys. Chem. Lett. 2016, 7, 1901−1906

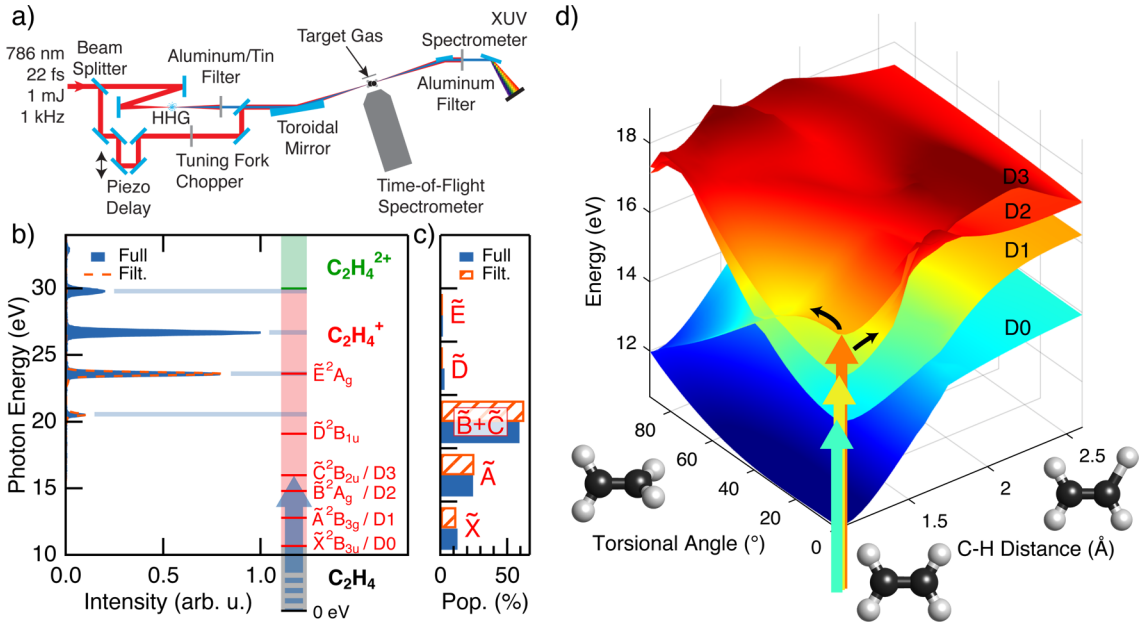

Figure 1. (a) Experimental setup. The high-order harmonic radiation is recombined with the fundamental IR (probe) pulses through a drilled mirror. (b) The excitation spectrum consisting of photons with energies in the extreme-ultraviolet spectral range. An insertable tin (Sn) filter allows us to switch between the full (solid blue) and a filtered (dashed orange line) spectrum. The inset shows the cationic states (red) that are reachable with the given photon energies.[21] (c) Initial population of the states calculated for the applied spectra.[22] (d) Calculated potential energy surfaces for the cation ground (D0) and the first three excited states (D1, D2, and D3) geometry-optimized on D0 along constrained values for the dihedral angle and C−H stretch coordinate using LR-TDDFT/PBE0 with a 6-31G** basis set and the quantum chemistry program Gaussian-G09.[23] The reference zero energy is the ground-state energy of the neutral molecule in its equilibrium geometry.

dissociation channels leading to loss of H or H_2. Our experiment gives access to signatures of the excited wave packet along its relaxation pathway on a femtosecond time scale that we use to identify key configurations at which CIs occur. Special attention is paid to the possibility of controlling the dissociation dynamics.

We record delay-dependent ion mass spectra in our experiment carried out at the attoline of ETH Zurich[24] (Figure 1a). For the excitation step, we employ attosecond pulse trains with photon energies in the range of 20−30 eV (Figure 1b). The attosecond pulse train is composed of pulses with a time duration between 300 and 400 as under an 11 fs envelope.[25] An additional tin (Sn) filter inserted into the XUV beam allows us to limit the range to 20−24.5 eV. We use the two excitation spectra to ionize ethylene molecules from the ground state to different excited states of the cation $C_2H_4^+$ and at the same time be able to exclude the role of double ionization to $C_2H_4^{2+}$ from the observed dynamics. A time-delayed IR probe pulse (22 ± 2 fs of duration) of variable intensity (photon energy 1.6 eV) probes the evolution of the dynamics through changes in the fragment ion yields. The cross-correlation between pump and probe obtained by ionizing Ar atoms is 24.5 ± 2 fs (see the Supporting Information). It is worth noting that the use of attosecond pulses enables resolving coherent dynamics that unfold on time scales faster than a femtosecond (see Figures 1 and 2 in the Supporting Information).

The ionization of ethylene launches molecular dynamics on different cationic states that can be represented by nuclear wave packets evolving on the PES toward the stable cation ground state or toward dissociative channels (Figure 1d). The asymptotic outcome of these dynamics is visible as static ion yield that exhibits three dominant peaks corresponding to the cation $C_2H_4^+$ and the largest fragments $C_2H_3^+$ and $C_2H_2^+$. This dominant structure is accompanied by the smaller fragments with 2 orders of magnitude lower peak heights (Figure 2a). The additional strong peak at 4 u stems from ionization of He used as buffer gas with a He:C_2H_4 ratio of 10:1. Starting from the tabulated values for the cross sections of ethylene for monochromatic light,[22,26] we estimate the initial state populations for our XUV spectra of Figure 1b. We find more than 95% of the total population is confined to the cation ground state $\tilde{X}\ ^2B_{3u}$ and the first three excited states $\tilde{A}\ ^2B_{3g}$, $\tilde{B}\ ^2A_g$, and $\tilde{C}\ ^2B_{2u}$ (Figure 1c).

The addition of the IR probe pulse at a defined delay after excitation allows us to interact with the molecular dynamics on a femtosecond time scale. The IR photons may transfer the nuclear wave packet between neighboring states or influence its branching ratio around CIs and thus change the asymptotic fragment yields. Figure 2b shows the IR-induced change in the ion yields relative to the XUV-only yields as a function of the pump−probe delay for an IR peak intensity of 2.5×10^{12} W/cm^2, a delay step size of 2 fs, and accumulation over 20 000 laser shots per data point. For positive delays, the IR pulse arrives after the XUV pulse. We observe a variety of dynamics visible as modulations in the yields within the first 60 fs after excitation. We carefully checked that the observed features are largely independent of the IR probe intensity as well as the exact excitation spectrum (see the Supporting Information). A decreasing IR probe intensity results in a decreased strength of the features but does not alter their timing. We exclude the contribution of dicationic states in the excitation step by applying the Sn filter in the XUV beam which effectively limits the spectrum far below the second ionization potential of ethylene and by comparing the results with the ones using the full XUV spectrum.

DOI: 10.1021/acs.jpclett.6b00646
J. Phys. Chem. Lett. 2016, 7, 1901−1906

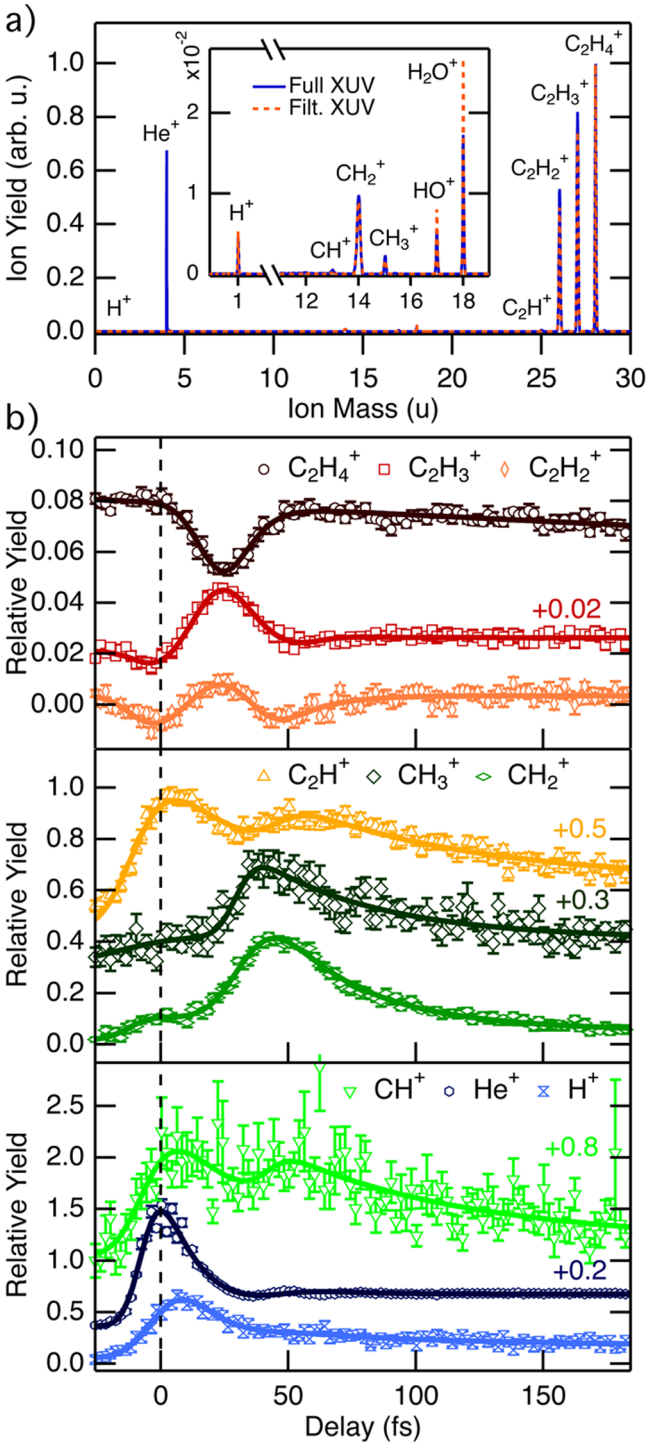

Figure 2. (a) Measured ion spectrum resulting from excitation of ethylene with the full and filtered XUV spectra (Figure 1b). The inset shows the yields of the smaller fragments. (b) Delay-dependent IR-induced relative change of the ion yields. For clarity, some curves have been shifted by an arbitrary vertical offset which is indicated next to the data points. The error bars represent the standard error of the mean of 10 measurements.

We present all measured ion yields that show a dynamic behavior plotted as markers together with their respective fit that we use to extract the delay position of the maximum yield. These fits are based on the sum of a minimal number of exponentially modified Gaussian (EMG) functions[27] as analytic approximation to a model that has recently been introduced for the description of ultrafast fragmentation dynamics of ethylene.[20] We estimate the error of the delays based on the fitting error for the position of the Gaussian part of the convoluted fitting function to be ±3 fs for all species except for CH^+, where it increases to ±10 fs because of the noise level of the data for this fragment.

We concentrate our analysis on two main features in the observed yields. One is the correlated dynamics in the $C_2H_4^+$, $C_2H_3^+$, and $C_2H_2^+$ ion yields that are closely linked through the dissociation channels leading to the loss of one or two hydrogen atoms. The other feature is the evolution of the CH_3^+, CH_2^+, and CH^+ yields resulting from the breakup of the C−C bond. We observe a comparable behavior of these monocarbon fragments at delays around 40 fs. Among them, the presence of CH_3^+ fragments is particularly interesting because it is an unambiguous signature of the ethylene−ethylidene isomerization that is supposed to play an important role in the dynamics leading to dissociation to $C_2H_2^+ + H_2$.[2] The maximum of the CH_3^+ yield was previously analyzed by applying an extended rate model to extract an isomerization time of 50 ± 25 fs.[20] Profiting from our accurate time-zero calibration,[28] the time resolution, and the good statistics of our measurements, we are able to extract a more precise upper bound for the isomerization time of 30 ± 3 fs, defined as the time that the nuclear wave packet needs to reach a region of the potential energy surface where the isomer population probability is maximum. It is extracted by fitting the CH_3^+ yield with a delayed exponential decay convoluted with the instrument response.[20] In the raw data it corresponds to the time position of the peak at 40 fs in Figure 2b.

Another important process is the loss of one or two H atoms after photoexcitation of the molecule. The two responsible channels, $C_2H_4^+ \rightarrow C_2H_3^+ + H$ and $C_2H_4^+ \rightarrow C_2H_2^+ + H_2$, exhibit similar thresholds from the cation ground state of 2.70 and 2.62 eV, respectively,[29] which are also consistent with the PBE0/DFT values of 2.75 and 2.70 eV. A signature of these channels in the XUV-only ion spectrum is found in the two dominant peaks at masses of 26 u ($C_2H_2^+$) and 27 u ($C_2H_3^+$) (Figure 2a) that show narrow correlated features in the delay-dependent ion yields. At a delay around 25 fs, the $C_2H_4^+$ yield decreases, which coincides with an increase in the $C_2H_3^+$ and $C_2H_2^+$ yields. This suggests that it takes the cation approximately 25 fs after excitation to reach a geometrical configuration where the IR is more likely to promote the loss of an additional H or H_2 fragment with associated bleaching of the $C_2H_4^+$ yield. This picture supposes ultrafast relaxation mechanisms between the first three excited states, which is in agreement with previous theoretical predictions on the relaxation time scales.[8]

To gain further insight into the dynamics of the excited ethylene cation, we perform trajectory surface hopping (TSH) calculations after excitation of the ethylene cation based on time-dependent density functional theory in a linear response formulation (LR-TDDFT).[30,31] Simulations were carried out with the Newton.X package[32] interfaced with G09 for the calculation of the electronic properties. We use the 6-31G** basis set on the LR-TDDFT/PBE0 level of theory and 100 TSH trajectories per excited state (see Computational Methods in the Supporting Information for more details). Initial geometries and velocities are obtained from Wigner distributions of the neutral ethylene in its ground state. We concentrate our analysis on the four lowest cationic states and verify a good agreement between their representation as spectroscopic states

DOI: 10.1021/acs.jpclett.6b00646
J. Phys. Chem. Lett. 2016, 7, 1901−1906

($\tilde{X}$, $\tilde{A}$, $\tilde{B}$, and $\tilde{C}$) based on neutral ethylene and the states used in the calculation (D0, D1, D2, and D3) for the ethylene cation.

Figure 1d shows the calculated PES of the cation ground and the first three excited states, geometry-optimized on the ground state as a function of the torsional angle and one C−H stretch coordinate. From this static representation of the potential energy surface, efficient transitions between D1 and D0 are expected around three different CIs, located along the dihedral angle at 90°, along the C−H coordinate around 1.7 Å, and along the planar bridging coordinate (see the Supporting Information for the latter two). This finding is consistent with the previous theoretical studies of Sannen and co-workers,[2] predicting a CI along the C−H stretching coordinate, and of Joalland et al.,[8] describing two D1/D0 CIs, one of bridged planar geometry and the other twisted.

To complete this static picture, we also performed dynamic simulations using a trajectory surface hopping approach. The temporal evolution of the population on the different states following excitation on D3, D2, and D1 is shown in Figure 3a.

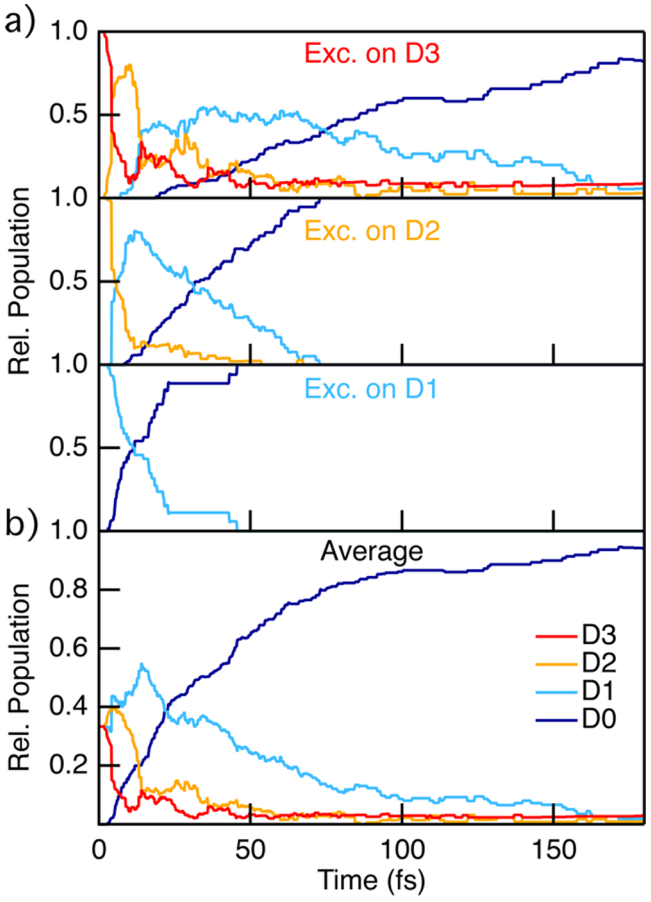

Figure 3. (a) Calculated population on the four lowest cationic states as a function of time after selective excitation to D1, D2, or D3. (b) The average population after simultaneous and equal excitation to D1, D2, and D3.

In Figure 3b, the average population of the first three excited states is shown assuming equal initial contributions. Our results are in good overall agreement with recent calculations using the AIMS method starting from the cation geometry[8] rather than from the neutral geometry as in present theoretical work. We find a fast relaxation of the majority of the initial population to the ground state within the first 50 fs after excitation. The averaged population on D1 reaches a distinct maximum after approximately 15 fs, consecutively decaying to the ground state.

It has been shown previously that CIs between the two lowest PES D1 and D0 of the ethylene cation are involved in the dynamics leading to the dissociation into $C_2H_3^+ + H$ and $C_2H_2^+ + H_2$.[1,2] The delay of 25 fs for the IR-induced change of the fragmentation channels is in good agreement with the time scale of relaxation to D1 observed in our simulations. Under the assumption that the branching into different channels happens around CIs between D1 and D0, the IR pulse probes the presence of the nuclear wave packet around these conical intersections. Thus, we can use the IR pulse in the experiment to precisely time how long it takes the excited wave packet to reach the responsible CI.

The distributions of C−H stretch coordinates and dihedral angles of all hopping events for transitions between different PESs together with the initial excitation geometry are shown in Figure 4a,b. We observe the largest C−H distances for the

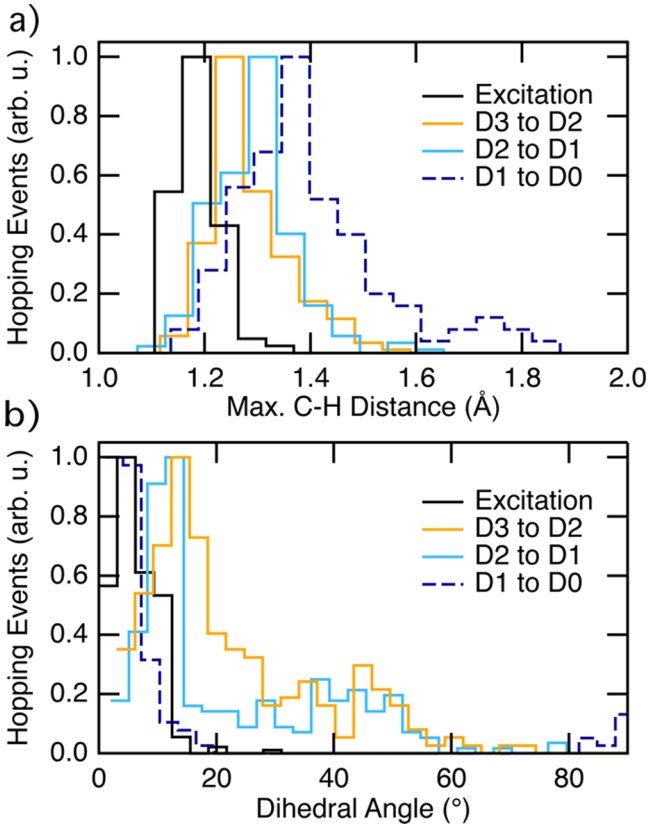

Figure 4. Hopping geometries for transitions between different states and the excitation geometries for comparison, shown for equal initial populations on D1, D2, and D3: (a) distribution of the maximal C−H distances per molecule and (b) distribution of the dihedral angles.

transitions from D1 to the cation ground state, reinforcing the assumption that this transition plays a central role in the dissociation channel leading to breakup of one C−H bond. For the dihedral angle, we observe a partitioning of the transition geometries to D0 around planar and 90° twisted geometries in contrast to the broad spread of dihedral angles from 0° to 60° observed for the transitions to D1 and D2. Here, the contribution around 90° twisted geometries uniquely stems from excitation to D3. This is also reflected in the timing, as at early stages, transitions to the ground state dominantly occur

DOI: 10.1021/acs.jpclett.6b00646
J. Phys. Chem. Lett. 2016, 7, 1901−1906

close to the initial planar geometry. Just after 30 fs, the twisted channel described by Joalland et al.[8] with a dihedral angle around 90° starts to play a role in the hopping to D0. We observe that a small number of trajectories, not statistically significant, leads to H or H_2 loss. It is worth noting that all these events occur in the ground state, not necessarily involving isomerization or bridging, and in the trajectories that have relaxed through a planar (either stretched or bridged) CI only (see the Supporting Information).

In summary, we presented investigations of the ultrafast photodissociation dynamics of the ethylene cation $C_2H_4^+$ excited by a XUV pulse train and probed with a delayed near-infrared pulse. The recorded delay-dependent fragment yields exhibit rich dynamics within the first 60 fs after excitation and thus represent evidence for the ultrafast response of the molecule. We observe a localized IR-induced enhancement in the $C_2H_3^+$ + H and $C_2H_2^+$ + H_2 channels after 25 fs that we attribute to wave packets on D1 reaching the conical intersection leading to the ground state D0. We demonstrate a possible route to obtain optical control of this excited-state dissociation channel by means of a delayed IR pulse at moderate intensities. We observe a maximum in the CH_3^+ ion yield as signature of the ethylene to ethylidene isomerization which allows us to refine the upper bound for the isomerization time to 30 ± 3 fs. Our measurements represent, to the best of our knowledge, the studies of fragmentation dynamics of the ethylene cation with the highest temporal resolution thus far. The temporal resolution of our experiment allows us to disentangle different dissociation mechanisms and connect previous complementary computational studies. We link our experimental findings to calculations using trajectory surface hopping based on a LR-TDDFT/PBE0 level of theory which permits us to access the relevant molecular configuration along the relaxation pathway. Our findings lift the experimental observations on the ultrafast dynamics of ethylene to a new level and will stimulate developments in their theoretical description. We were also able to identify three CIs involved, two of them possibly favoring H or H_2 elimination in the ground state.

■ ASSOCIATED CONTENT

Supporting Information

The Supporting Information is available free of charge on the ACS Publications website at DOI: 10.1021/acs.jpclett.6b00646.

Details on the experimental and computational methods, as well as extended experimental results (PDF)

Example of H-loss in one calculated trajectory (MPG)

Example of H_2-loss in one calculated trajectory (MPG)

■ AUTHOR INFORMATION

Corresponding Author

*E-mail: mlucchini@phys.ethz.ch.

Notes

The authors declare no competing financial interest.

■ ACKNOWLEDGMENTS

This research was supported by the NCCR MUST, funded by the Swiss National Science Foundation and the ETH Zurich Postdoctoral Fellowship Program.

■ REFERENCES

(1) Lorquet, J. C.; Sannen, C.; Raşeev, G. Dissociation of the Ethylene Cation: Mechanism of Energy Randomization. *J. Am. Chem. Soc.* **1980**, *102*, 7976−7977.

(2) Sannen, C.; Raşeev, G.; Galley, C.; Fauville, G.; Lorquet, J. C. Unimolecular Decay Paths of Electronically Excited Species. II. The C2H4+ Ion. *J. Chem. Phys.* **1981**, *74*, 2402−2411.

(3) Farmanara, P.; Stert, V.; Radloff, W. Ultrafast Internal Conversion and Fragmentation in Electronically Excited C2H4 and C2H3Cl Molecules. *Chem. Phys. Lett.* **1998**, *288*, 518−522.

(4) Tao, H.; Allison, T. K.; Wright, T. W.; Stooke, A. M.; Khurmi, C.; van Tilborg, J.; Liu, Y.; Falcone, R. W.; Belkacem, A.; Martinez, T. J. Ultrafast Internal Conversion in Ethylene. I. The Excited State Lifetime. *J. Chem. Phys.* **2011**, *134*, 244306.

(5) Ben-Nun, M.; Martínez, T. J. Ab Initio Molecular Dynamics Study of Cis-trans Photoisomerization in Ethylene. *Chem. Phys. Lett.* **1998**, *298*, 57−65.

(6) Martínez, T. J. Insights for Light-driven Molecular Devices from Ab Initio Multiple Spawning Excited-state Dynamics of Organic and Biological Chromophores. *Acc. Chem. Res.* **2006**, *39*, 119−126.

(7) Levine, B. G.; Martínez, T. J. Isomerization Through Conical Intersections. *Annu. Rev. Phys. Chem.* **2007**, *58*, 613−634.

(8) Joalland, B.; Mori, T.; Martínez, T. J.; Suits, A. G. Photochemical Dynamics of Ethylene Cation $C_2H_4^+$. *J. Phys. Chem. Lett.* **2014**, *5*, 1467−1471.

(9) Schoenlein, R.; Peteanu, L.; Mathies, R.; Shank, C. The First Step in Vision: Femtosecond Isomerization of Rhodopsin. *Science* **1991**, *254*, 412−415.

(10) Gonzalez-Luque, R.; Garavelli, M.; Bernardi, F.; Merchan, M.; Robb, M. A.; Olivucci, M. Computational Evidence in Favor of a Two-state, Two-mode Model of the Retinal Chromophore Photoisomerization. *Proc. Natl. Acad. Sci. U. S. A.* **2000**, *97*, 9379−9384.

(11) Polli, D.; Altoè, P.; Weingart, O.; Spillane, K. M.; Manzoni, C.; Brida, D.; Tomasello, G.; Orlandi, G.; Kukura, P.; Mathies, R. A.; et al. Conical Intersection Dynamics of the Primary Photoisomerization Event in Vision. *Nature* **2010**, *467*, 440−443.

(12) Satzger, H.; Townsend, D.; Zgierski, M. Z.; Patchkovskii, S.; Ullrich, S.; Stolow, A. Primary Processes Underlying the Photostability of Isolated DNA Bases: Adenine. *Proc. Natl. Acad. Sci. U. S. A.* **2006**, *103*, 10196−10201.

(13) Barbatti, M.; Aquino, A. J. a.; Szymczak, J. J.; Nachtigallová, D.; Hobza, P.; Lischka, H. Relaxation Mechanisms of UV-photoexcited DNA and RNA Nucleobases. *Proc. Natl. Acad. Sci. U. S. A.* **2010**, *107*, 21453−21458.

(14) Ben-Nun, M.; Quenneville, J.; Martínez, T. J. Ab Initio Multiple Spawning: Photochemistry from First Principles Quantum Molecular Dynamics. *J. Phys. Chem. A* **2000**, *104*, 5161−5175.

(15) Kim, M. H.; Leskiw, B. D.; Suits, A. G. Vibrationally Mediated Photodissociation of Ethylene Cation by Reflectron Multimass Velocity Map Imaging. *J. Phys. Chem. A* **2005**, *109*, 7839−7842.

(16) Kim, M. H.; Leskiw, B. D.; Shen, L.; Suits, A. G. Vibrationally Mediated Photodissociation of C2H4+. *J. Phys. Chem. A* **2007**, *111*, 7472−7480.

(17) Stert, V.; Lippert, H.; Ritze, H. H.; Radloff, W. Femtosecond Time-resolved Dynamics of the Electronically Excited Ethylene Molecule. *Chem. Phys. Lett.* **2004**, *388*, 144−149.

(18) Kosma, K.; Trushin, S. A.; Fuss, W.; Schmid, W. E. Ultrafast Dynamics and Coherent Oscillations in Ethylene and Ethylene- d 4 Excited at 162 nm. *J. Phys. Chem. A* **2008**, *112*, 7514−7529.

(19) Allison, T. K.; Tao, H.; Glover, W. J.; Wright, T. W.; Stooke, A. M.; Khurmi, C.; van Tilborg, J.; Liu, Y.; Falcone, R. W.; Martínez, T. J.; et al. Ultrafast Internal Conversion in Ethylene. II. Mechanisms and Pathways for Quenching and Hydrogen Elimination. *J. Chem. Phys.* **2012**, *136*, 124317.

(20) Tilborg, J. V.; Allison, T. K.; Wright, T. W.; Hertlein, M. P.; Falcone, R. W.; Liu, Y.; Merdji, H.; Belkacem, A. Femtosecond Isomerization Dynamics in the Ethylene Cation Measured in an EUV-pump NIR-probe Configuration. *J. Phys. B: At., Mol. Opt. Phys.* **2009**, *42*, 081002.

DOI: 10.1021/acs.jpclett.6b00646
J. Phys. Chem. Lett. 2016, 7, 1901−1906

(21) Mackie, R. A.; Scully, S. W. J.; Sands, A. M.; Browning, R.; Dunn, K. F.; Latimer, C. J. A Photoionization Mass Spectrometric Study of Acetylene and Ethylene in the VUV Spectral Region. *Int. J. Mass Spectrom.* **2003**, *223−224*, 67−79.
(22) Ibuki, T.; Cooper, G.; Brion, C. Absolute Dipole Oscillator Strengths for Photoabsorption and the Molecular and Dissociative Photoionization of Ethylene. *Chem. Phys.* **1989**, *129*, 295−309.
(23) Frisch, M. J.; Trucks, G. W.; Schlegel, H. B.; Scuseria, G. E.; Robb, M. A.; Cheeseman, J. R.; Scalmani, G.; Barone, V.; Mennucci, B.; Petersson, G. A. et al. *Gaussian 09*, revision A.01. Gaussian, Inc.: Wallingford, CT, 2009.
(24) Locher, R.; Lucchini, M.; Herrmann, J.; Sabbar, M.; Weger, M.; Ludwig, A.; Castiglioni, L.; Greif, M.; Hengsberger, M.; Gallmann, L.; et al. Versatile Attosecond Beamline in a Two-foci Configuration for Simultaneous Time-resolved Measurements. *Rev. Sci. Instrum.* **2014**, *85*, 013113.
(25) Lucchini, M.; Herrmann, J.; Ludwig, A.; Locher, R.; Sabbar, M.; Gallmann, L.; Keller, U. Role of Electron Wavepacket Interference in the Optical Response of Helium Atoms. *New J. Phys.* **2013**, *15*, 103010.
(26) Berkowitz, J. *Atomic and Molecular Photoabsorption*; Elsevier: Amsterdam, 2015; pp 442−458.
(27) Kalambet, Y.; Kozmin, Y.; Mikhailova, K.; Nagaev, I.; Tikhonov, P. Reconstruction of Chromatographic Peaks Using the Exponentially Modified Gaussian Function. *J. Chemom.* **2011**, *25*, 352−356.
(28) Herrmann, J.; Lucchini, M.; Chen, S.; Wu, M.; Ludwig, A.; Kasmi, L.; Schafer, K. J.; Gallmann, L.; Gaarde, M. B.; Keller, U. Multiphoton Transitions for Delay-zero Calibration in Attosecond Spectroscopy. *New J. Phys.* **2015**, *17*, 013007.
(29) Stockbauer, R.; Inghram, M. G. Threshold Photoelectron-photoion Coincidence Mass Spectrometric Study of Ethylene and Ethylene-d4. *J. Chem. Phys.* **1975**, *62*, 4862−4870.
(30) Tapavicza, E.; Tavernelli, I.; Rothlisberger, U. Trajectory Surface Hopping within Linear Response Time-Dependent Density-Functional Theory. *Phys. Rev. Lett.* **2007**, *98*, 023001.
(31) Tapavicza, E.; Tavernelli, I.; Rothlisberger, U.; Filippi, C.; Casida, M. E. Mixed Time-dependent Density-functional Theory/Classical Trajectory Surface Hopping Study of Oxirane Photochemistry. *J. Chem. Phys.* **2008**, *129*, 124108.
(32) Barbatti, M.; Ruckenbauer, M.; Plasser, F.; Pittner, J.; Granucci, G.; Persico, M.; Lischka, H. Newton-X: a Surface-hopping Program for Nonadiabatic Molecular Dynamics. *Wiley Interdiscip. Rev. Comput. Mol. Sci.* **2014**, *4*, 26−33.

DOI: 10.1021/acs.jpclett.6b00646
J. Phys. Chem. Lett. 2016, 7, 1901−1906